Second harmonic generation (SHG) in pentacene thin films grown by matrix assisted pulsed laser evaporation (MAPLE)

Iulian Ionita, Adrian Bercea, Simona Brajnicov, Andreea Matei, Valentin Ion, Valentina Marascu, Bogdana Mitu, Catalin Constantinescu

Second harmonic generation (SHG) in pentacene thin films grown by matrix assisted pulsed laser evaporation (MAPLE)

*Iulian IONITA[1], Adrian BERCEA[2,3], Simona BRAJNICOV[2,4], Andreea MATEI[2], Valentin ION[2], Valentina MARASCU[1,2], Bogdana MITU[2], *Catalin CONSTANTINESCU[3]*

[1] *University of Bucharest, Faculty of Physics, Bd. Atomistilor nr. 405, RO-077125 Magurele (Bucharest), Romania*

[2] *INFLPR - National Institute for Lasers, Plasma, and Radiation Physics, Bd. Atomistilor nr. 409, RO-077125 Magurele (Bucharest), Romania*

[3] *University of Limoges, CNRS, IRCER UMR 7315, 12 rue Atlantis, F-87000 Limoges, France*

[4] *University of Craiova, Faculty of Sciences, Str. A.I. Cuza nr. 13, RO-200585 Craiova, Romania*

Abstract

Thin films of pentacene, *i.e.* a polycyclic hydrocarbon consisting of five linearly-fused benzene rings, are grown on silicon and quartz (SiO_2) substrates by matrix assisted pulsed laser evaporation (MAPLE) and by using toluene as a frozen matrix (melting point: −95 °C). The thin film samples are subsequently investigated for their optical, morphological and chemical structure, *i.e.* by Fourier transform infrared spectroscopy (FTIR), scanning electron microscopy (SEM), atomic force microscopy (AFM), and spectroscopic-ellipsometry (SE). Due to its highly conjugated aromatic behaviour, pentacene exhibits semiconductor properties and has been shown to generate excitons upon absorption of ultra-violet (UV) or visible light. Here, we study the excited state dynamics of pentacene, in bulk and as thin films, after optical excitation, by using femtosecond (fs) time-resolved second harmonic generation (SHG). A pulsed femtosecond Ti:sapphire laser (80 MHz repetition rate, 800 nm, 100 fs) is employed to demonstrate the SHG potential of such polycyclic aromatic hydrocarbon simple molecule. The substrates used in studying the films are inert and non-interacting, known to deliver no noteworthy contribution to the SHG signal. Therefore, the pure response of pentacene to the electronic excitation can be resolved in contrast to the measurements on SiO_2. Finally, a comparative discussion of our results is made with respect to literature. This study provides important insights on the excited states dynamics of pentacene, an essential step for understanding the photophysics of simple, linearly-fused arenes.

Keywords: *pentacene, organic semiconductor, thin film, photophysics, second harmonic generation.*

1. Introduction

The need for "use-and-throw" materials, for cost-efficient eco-friendly sensors, electronics, and single use devices, led to a significant growth in the field of organic and biodegradable materials. Organic electronics comes with advantages such as reduced costs, simple processing and efficiency, low processing temperatures, in addition to the ecological reasons [1]. The nonlinear optical (NLO) capabilities of organic thin films have been

* Electronic mail: *catalin.constantinescu@unilim.fr*

extensively studied in the last decades, targeting applications such as spectroscopy and imaging, second harmonic generation (SHG), electro-optic modulation (EOM) for specific, aimed applications, *e.g.* in medicine and optoelectronics [2-5].

A dark blue powder in bulk, pentacene is a polycyclic aromatic hydrocarbon (i.e. a linear *acene*), a small molecule exhibiting p-type organic semiconducting properties with high field effect mobility due to the highly π-conjugated electronic structure [6]. Pentacene and some of its derivatives were first synthesized in 1912 by chemists William Hobson Mills and Mildred May Gostling of the Northern Polytechnic Institute in London. More efficient synthetic methods were devised later on by Marschalk and by Allen and Gates, in the 1930s and 1940s, respectively. Modern synthetic methods have been devised in order to overcome the low solubility of pentacene in common organic solvents, which limits its deposition as films, and therefore its applications. Pentacene is well soluble in hot chlorinated benzenes, such as 1,2,4-trichlorobenzene, from which it can be recrystallized to form platelets. The first crystal structure determination of pentacene molecular crystals was reported in 1961: "Crystals of pentacene obtained by crystallization from trichlorobenzene consisted of extremely thin deep violet-blue leaflets, with only the (001) face developed. Attempts to grow thicker specimens by recrystallization from trichlorobenzene in an atmosphere of carbon dioxide yielded only similar very thin plate-like crystals." [5]. This experimental study allowed researchers for the first time to accurately determine the molecular dimensions of the pentacene molecule: ~14 Å in length, and the C-C bond that range from 1.381 to 1.464 Å in length. Single crystals of pentacene can be grown either from organic solvents or by various techniques, such as the metal-organic vapor-phase epitaxy (MOVPE) [5-7]. The peculiar packing adopted by the pentacene molecules in a crystalline form is noteworthy, *i.e.* aligned in parallel along the *a* and *b* crystal axes of the unit cell, thereby forming molecular monolayers in the *a*, *b* plane. The monolayers are characterized by *d*-spacing of 14.1, 14.5 or 15.4 Å, depending upon the method of crystallization adopted. Pentacene is the most studied organic semiconductor used for organic field-effect transistor (o-FET) systems, with a high application potential due to a hole mobility in OFETs of up to 5–6 $cm^2 V^{-1} s^{-1}$ in highly polycrystalline films, which exceeds that of amorphous silicon [7-9]. It was also tested in organic light-emitting diode (LED), photovoltaic devices, and its derivatives have been examined as potential dichroic dyes [10-11]. SHG has already been used as a method of probing for the device operation based on pentacene use in FET [12, 13]. However, due to

the fact that the compound generates excitons upon absorption of ultra-violet (UV) or visible light, this makes it very sensitive to oxidation and therefore limits its use [14]. Upon deposition on any insulating substrate, pentacene molecules organize to form polycrystalline films. The most common deposition techniques for growing pentacene and similar molecules as thin films are chemically vapour deposition (CVD), cluster beam deposition (CBD), vacuum evaporation, pentacene precursors, spin coating, dropcasting, blade coating and inkjet printing from solutions. Other non-conventional methods, such as pulsed laser deposition (PLD) and laser-induced forward transfer (LIFT) have also been presented in literature [14-35]. However, solution processed thin film devices typically require a multi-layer construction in which successive layers are deposited from solvents of opposite polarity such that the deposition of each new film does not damage the preceding layer. Here, we report on the morphological, chemical and optical properties of pentacene thin films deposited by matrix assisted pulsed laser evaporation (MAPLE).

MAPLE is a modified pulsed laser deposition procedure specially created for delicate materials such as polymers, proteins, biomaterials, and soft materials, or molecules with complicated structure [36-46]. It involves the homogenization of the interest material (solubilisation or suspension of the guest molecules) in a matrix (*i.e.* a solvent, miscible liquid or gel), the usual concentration of the guest material being 0.1–4 wt%. The mixture is subsequently solidified (*i.e.* frozen to liquid nitrogen) in order to create a system that can be used as a target. When the target inside a vacuum system is irradiated by a low-fluence pulsed laser beam (typically in the range of 0.1 – 0.7 J/cm^2), the matrix evaporates and is pumped out of the system, whereas the guest molecules are collected on a substrate. MAPLE requires a matrix highly absorbing at the wavelength of the laser beam, while a relatively low absorption by the guest material is preferred. On the other hand, other ejection mechanisms may also be involved during the laser–target interaction. Photo-chemical reactions between the matrix and guest materials need to be avoided or considerably reduced, *e.g.* by preferring non-halogenated solvents to halogenated ones, or by using solvents that have linear and/or branched instead of only cyclic catenae, whenever possible. Since the film is not in contact with any solvents after the deposition, MAPLE can be used for obtaining combinations of layers and as part of devices, for which no compatible solvent exists. The advantages of this soft laser-processing method involve: well-controlled film thickness and adherence, together with the possibility of growing simple or hybrid

multi-structures, *e.g.* organic/organic *vs.* organic/inorganic, simply by using a multi-compartmented target design [45].

In this contribution, we study the influence of a pulsed femtosecond Ti:sapphire laser (80 MHz repetition rate, 800 nm, 100 fs) on pentacene in bulk and in MAPLE grown thin films, to demonstrate the SHG potential of such a polycyclic aromatic hydrocarbon simple molecule. The substrates used in studying the films are inert and non-interacting, known to deliver no noteworthy contribution to the SHG-signal. This study provides important insights on the excited states dynamics of pentacene, an essential step for understanding the photophysics of simple, linearly-fused arenes.

2. Experimental

2.1 Materials and thin film growth

Pentacene was acquired from Sigma-Aldrich and used "as provided". For the MAPLE experiments, we used 1wt % pentacene dissolved in toluene (melting point: −95 °C), frozen down by liquid nitrogen cooled system on a copper target holder (*figure 1a*), and maintained solid during laser irradiation. The laser fluence used was in the range of 0.2 –0.4 J/cm² at 266 nm wavelength (the fourth harmonic of a Nd:YAG - Surelite II - Continuum Company). The repetition rate was set at 10 Hz (maximum available). The depositions took place in vacuum at an initial pressure of $1x10^{-5}$ mbar, based on the thermodynamics and kinetics of the phase transition simulations, and previous studies on the dynamics of the ablation process in order to minimize photochemical-induced damage from direct interaction with the intense laser [41, 46]; the pressure slightly increased (>$5x10^{-5}$ mbar) during irradiation due to solvent evaporation. Thin films have been grown on silicon and on quartz substrates, corresponding to 36 000 – 72 000 pulses. The target was rotated while the beam scanned its surface during deposition, with the substrate placed in front of the target (4 cm) and parallel to it. The deposition rate was determined by a quartz crystal microbalance (QCM) device.

2.2 Chemical, morphological & structural analysis, SHG properties

Atomic force microscopy (AFM) ("XE-100" setup produced by Park Systems) and scanning electron microscopy (SEM) ("Quanta ESEM FEG 450" produced by FEI) have been employed to study the thin films surface morphology. Optical measurements performed by spectroscopic ellipsometry (SE) technique ("V-VASE" setup produced by J.A. Wollam) acquired the data points in 350-1700 nm range with a step of 2 nm and at 65° angle of the

incidence. Fourier transform infrared absorption (FTIR) spectra of the pentacene thin films grown by MAPLE are compared to dropcasted films, achieved in transmission in the range 400 – 4000 cm^{-1} with 4 cm^{-1} resolution ("FT/IR-6300 FT-IR Spectrometer" produced by Jasco). The setup for SHG employed a femtosecond laser, since the SHG induced by femtosecond laser beam irradiation instead of a nanosecond Nd:YAG laser is superior due to the higher electric field induced at sample level for a lower deposed energy. This means that the efficiency of SHG is higher and structural changes induced during the beam irradiation are lees probable to happen. The femtosecond pulsed beam was delivered by a Ti:sapphire oscillator ("Tsunami", produced by Spectra Physics) operating at 80 MHz and 800 nm central wavelength, with 100 fs pulse duration at the sample level. The power of the incident beam was adjusted by a combination of half-wave plate and Glan-Thompson polarizer. The average beam power was varied in the range 0–400 mW. The beam was focused onto the analysed sample by a 20X objective lens (5 µm spot size). Both reflected SHG and reflected NIR light have been collected by the same lens and sent through a slit of a short focal distance spectrograph coupled to a thermoelectrically cooled intensified charge-coupled device (iCCD) camera (developed by ANDOR, an Oxford Instruments Group). Although the spectrograph separates radiation depending on the wavelength (400 nm versus 800 nm in our case), the very low ratio between the intensities of both types of radiation require the use of a several IR cut filters before spectrograph entrance. The detection system spectrograph-camera is less efficient and slower than a filter-photomultiplier system but it is more reliable when measuring a very low signal on a high background.

3. Results and discussion

Although pentacene is well soluble in hot chlorinated benzenes, it is only slightly soluble in common organic solvents (*e.g.* simple arenes) leading to very low concentrations [47]. Furthermore, the pentacene molecule is very sensitive to oxygen especially when dissolved, slowly degrading upon exposure to air and light. Vacuum-deposited pentacene films usually contain polycrystalline crystallites and amorphous phase. The structure of pentacene films depends on the deposition temperature and evolves with the thickness. X-ray diffraction of polycrystalline pentacene films reveals that crystallites consist of both thin film phase and bulk phase with interlayer spacing *d* of 15.4 Å and 14.5 Å, respectively. Past studies suggested that the thin film phase nucleates on the substrate initially and the

nucleation of bulk phase increases obviously beyond a certain thickness (~100 nm), value that is known to decrease with increasing deposition temperature [34, 48, 49]. Therefore, our approach by using the MAPLE technique eliminates these drawbacks. Photochemical and oxidation effects are reduced to a minimum due to the low temperature of the system, low concentration, and high vacuum employed during thin film deposition. We already shown that high-quality pentacene thin films of high crystallinity and low surface roughness can be produced by PLD without inducing chemical degradation of the molecules [14]. Here, we show that the deposition at 0.2 J/cm² laser fluence and at a concentration of 1 wt % pentacene in toluene, led to a mass deposition rate of 1.13 ng/cm² per pulse, as measured by the QCM device. Profilometry studies on such thin films revealed deposition rates between 0.04 and 0.6 Å/ pulse for using fluences in the range 0.2 – 0.4 J/cm². These results have been further corroborated with spectroscopic and morphology investigations.

3.1 Fourier-transform infrared spectroscopy

Comparative FTIR spectra for pentacene dropcast *vs.* MAPLE deposited films, for different used laser fluences, are presented in *figure 1b* (inset, upper left: the pentacene molecule). The band at 3040 cm^{-1} corresponds to the C-H stretching vibration of the ring. At 1623 cm^{-1} and 1434 cm^{-1} one can identify the C-C vibrations of the ring, and at 909 cm^{-1} and 841 cm^{-1}, the C-H vibrations in the ring. Other distinctive vibrations (960 cm^{-1} and 992 cm^{-1}) are also present in the recorded spectra (as compared to the "Advanced Electronic Packaging", edited by William D. Brown). At 732 cm^{-1} is identified the C-H out of plane bending vibration; the peak at 1116 cm^{-1} corresponding to the C-H out of plane and the one at 1296 cm^{-1} corresponding to the C-C stretching, are pentacene's "fingerprint" vibrations [50-57]. No significant oxidation effects are observed, but traces of toluene in the film are also identified, as reported elsewhere [58].

3.2 Atomic force microscopy and scanning electron microscopy

The AFM study revealed dense and compact surfaces, with features that vary in height between a few tens to hundreds of nanometres (*figure 2a*), with evenly distributed aggregates with sizes up to a few microns. The root mean square (RMS) roughness is 107 nm for a film deposited at 0.4 J / cm², at a thickness of about 400 nm. The given film thickness is an average value because pentacene molecules are organized in microcrystallites of

different sizes and order on the substrate. The so-called “thin-film phase” is dominant at room temperature deposition and for an average film thickness smaller than 50 nm. The “single crystalline phase” dominates at higher substrate temperatures and for a thickness above 150 nm. Both phases appear in films of with more than 150 nm thickness deposited at room temperature, while the “single crystalline phase” is best expressed for deposition temperatures above 100 °C. The morphology on top of the films is strongly dependent upon the preparation conditions of the films. SEM investigations also reveal that the films are uniform and compact, without cracks or pores, covering entirely the substrate (*figure 2b*), proving that the films are similar or superior when compared to other deposition techniques.

3.3 Spectroscopic-ellipsometry

The optical model used for theoretical calculation is composed by a stack of three different layers: the SiO_2 substrate, the pentacene thin film, and a top layer with high roughness. Each layer has different optical constants and thickness. For the SiO_2 layer, the optical constants are from literature [59]. The top rough layer is approximated to be made of 50% air and 50% pentacene, and the values of refractive index and extinction coefficient are calculated in the frame of the Bruggeman approximation [60]. Theoretical calculations of the optical constants in pentacene thin films are made in two steps. First, it is necessary to calculate the thickness of this layer and for this purpose, a simple Cauchy dispersion formula with Urbach tail, are used in the range of 900-1700 nm, where the material is supposed to be optically transparent. The thickness of sample was found to be d = 355.5 ± 1.2 nm with a roughness t = 39.2 ± 0.5 nm and a MSE value of 31.7. The Cauchy-Urbach formalism can be used just for wavelengths where the material is optically transparent or exhibits weak absorption. In order to fit the experimental data on the entire measured spectrum, it was necessary to find another formalist. The best fit is obtained by using a sum of four Gauss oscillators (*figure 3a*). One may observe a discrepancy between the experimental data points (green and blue line) and the theoretical curve (red lines) in UV range (350-400 nm), and the same behaviour is also observed in the infrared range (1100-1700 nm). This discrepancy may be explained by the presence of micrometric features of up to 1.5 microns at the surface, as it can be seen in the AFM and SEM images. The calculated oscillators’ parameters are presented in *table 1*, where “Amp” is the amplitude of oscillation, “En” is the centre energy

of oscillator, and "Br" is the broadening of the oscillator. Furthermore, in order to fit experimental data with the model, it is important to assume depolarization effects [61, 62]. In experimental data from optical methods based on light-polarization, the depolarization may occur. The depolarization originates from incoherent superposition of different polarization states transmitting or reflecting from the sample. The depolarization effects come either from the setup itself or/and from a measured structure (*figure 3b*). In short, the physical phenomena that generate partially polarized light are as follows: (a)-incident angle variation originating from focusing of the probe light, (b)-wavelength variation caused by the finite spectral resolution of the monochromator, (c)-surface light scattering caused by a large surface roughness of a sample, (d)-thickness inhomogeneity of layers in the structure, (e)-backside reflection in a thick substrate. The generated optical constants, as a function of wavelength, are presented in *figure 4*. The strange optical behaviour in near IR range come from misalignment in the experimental/theoretical curve, and not from intrinsic properties of the material. In the 400-1100 nm range, the values of refractive index (*figure 4a*) and extinction coefficient (*figure 4b*) are in good agreement with other reported values [63]. The single molecule has a HOMO-LUMO gap of about 1.1 eV as deduced from the Kohn-Sham eigenvalue differences. Here, the value of the band gap is approximated from the Tauc plot, *i.e.* $f(E)=(\alpha E)^2$, where α is the absorption coefficient, *i.e.* $\alpha=4\pi k/\lambda$ (*figure 5*). This value is found to be Eg~1.72 eV +/- 0.05 eV, in reasonable agreement with literature [64]. Finally, the transmission spectrum (*figure 6*) reveals that the films are 60% to 80% transparent in the range of 900-1700 nm.

3.4 Second harmonic generation by pentacene thin films

Lack of inversion symmetry in a nonlinear medium is a necessary prerequisite for the occurrence of a second-order nonlinearity. However, the isolated pentacene molecule as well as pentacene crystals which exhibit a triclinic symmetry are nearly centrosymmetric. The second-order nonlinearity originates in pentacene films from the lack of inversion symmetry at the surfaces of the crystallites and is practically independent of the structure and morphology of the films [65-67]. The deformation mechanisms of molecular crystals and thin films combine characteristics of metals, liquid crystals and polymers. They tend to be soft like polymers, and their anisotropic molecular conformation, low molecular weight, weak inter-molecular interactions and lack of physical entanglements allow for significant

molecular rotations - like in liquid crystals. The high degree of long range order present in thin films and single crystals also allows for the presence of well-defined lattice defects [67].

The damage threshold value for pentacene is very high compared with other films of organic molecules and very important for their application in measurements of pulse duration of femtosecond pulses. First, we tested that the pentacene powder (bulk) gives a reasonable SHG signal at a chosen incident power without any changes during laser irradiation (*figure 7*), as this is a strong feature compared to other organic samples that may easily induce a violent decomposition and even burning under a focused laser beam. The nonlinear behaviour in the spectrum of light emitted by the pentacene nanolayer under femtosecond laser beam irradiation (*figure 8*) is highlighted by the regular shape of the emission band. Compared to SHG measurements of other organic layers made by the same experimental set-up [3, 68, 69] we can underline two main features of the pentacene layer: stronger SHG signal and higher resistance to the deposed energy by laser beam. Finally, we tested the dependence of the SHG intensity versus the incident beam power. The results are also shown in *figure 8*. We used squared power on abscissa in order to test the expected linearity $I(2\omega) \sim I2(\omega)$. The slope of fitting line, that is proportional to susceptibility, can be used to compare different samples measured with the same set-up in order to improve the experimental conditions of sample fabrication.

To explain the SHG efficiency for the centrosymmetrical pentacene films we have to assume that the distortion at the grain boundaries of the polycrystalline thin film is responsible for the SHG, *i.e.* to consider the size of the boundaries of the films to understand the different SHG efficiencies. Therefore, the efficiency of SHG is independent of the microscopic configuration.

4. Conclusion

Thin films of pentacene are grown by matrix-assisted pulsed laser evaporation. The films are uniform, dense and without pores or cracks, with uniformly distributed aggregates that can be observed at the surface. The refractive index of the films, as it was measured in the 400 – 1000 nm wavelength range, varies between 1.78 and 1.93 with a maximum in the UV region. The value of band gap was found to be Eg~1.72 eV +/- 0.05 eV, which is in reasonable agreement with literature. The efficiency of second harmonic generation is independent of the microscopic configuration and the morphological structure, but depends

upon the size of the surface and of the domains themselves. The nonlinear investigations reveal that the films exhibit second harmonic generation capabilities, making them suitable for applications organic optoelectronics.

Acknowledgements

This work was partially supported by grant of the Romanian National Authority for Scientific Research and Innovation, CNCS – UEFISCDI, project number PN-III-P2-2.1-PED-2016-0221 (contract PED 94/2017) – "IPOD".

The authors thank Eloise HYVERNAUD, Pierre CARLES and the CARMALIM team for their help in investigating the morphology of the thin film samples, and acknowledge the fruitful discussions with Frederic DUMAS-BOUCHIAT and Corinne CHAMPEAUX.

References

[1] M. Irimia-Vladu, E. D. Głowacki, G. Schwabegger, L. Leonat, H. Zekiye Akpinar, H. Sitter, S. Bauer, N. S. Sariciftci; "*Natural resin shellac as a substrate and a dielectric layer for organic field-effect transistors*"; Green Chemistry 15 (2013) 1473-1476; http://dx.doi.org/10.1039/c3gc40388b

[2] Y. Yan, Y. Yuan, B. Wang, V. Gopalan, N.C. Giebink; "*Sub-wavelength modulation of $\chi^{(2)}$ optical nonlinearity in organic thin films*"; Nature Communications 8 (2017) 14269; http://dx.doi.org/10.1038/ncomms14269

[3] C. Constantinescu, A. Matei, V. Ion, B. Mitu, I. Ionita, M. Dinescu, C.R. Luculescu, C. Vasiliu, A. Emandi; "*Ferrocene carboxaldehyde thin films grown by matrix-assisted pulsed laser evaporation for non linear optical applications*"; Applied Surface Science 302 (2014) 83–86; http://dx.doi.org/10.1016/j.apsusc.2013.11.147

[4] R.W. Boyd, "*Nonlinear Optics*", third ed., Academic Press, Elsevier, Oxford, UK, 2008, ISBN 978-0-12-369470-6

[5] R.B. Campbell, J.M. Robertson, J. Trotter; "*The crystal and molecular structure of pentacene*"; Acta Crystallographica 14 (1961) 705-711; http://dx.doi.org/10.1107/S0365110X61002163

[6] C. Pramanik, G.P. Miller; "*An Improved Synthesis of Pentacene: Rapid Access to a Benchmark Organic Semiconductor*"; Molecules 17 (2012) 4625-4633; http://doi.org/10.3390/molecules17044625

[7] R. Ruiz, D. Choudhary, B. Nickel, T. Toccoli, K.C. Chang, A.C. Mayer, P. Clancy, J.M. Blakely, R.L. Headrick, S. Iannotta, G.G. Malliaras; "*Pentacene Thin Film Growth*"; Chemistry of Materials 16 (2004) 4497-4508; http://dx.doi.org/10.1021/cm049563q

[8] C.K. Song, B.W. Koo, S.B. Lee, D.H. Kim; "*Characteristics of Pentacene Organic Thin Film Transistors with Gate Insulator Processed by Organic Molecules*"; Japanese Journal of Applied Physics 41 (2002) 2730–2734; http://doi.org/10.1143/JJAP.41.2730

[9] S.C.B. Mannsfeld, A. Virkar, C. Reese, M.F. Toney, Z. Bao; "*Precise Structure of Pentacene Monolayers on Amorphous Silicon Oxide and Relation to Charge Transport*"; Advanced Materials 21 (2009) 2294–2298; http://doi.org/10.1002/adma.200803328

[10] M.V.M. Rao, T.S. Huang, Y.K. Su, Y.T. Huang; "*Fullerene and pentacene as a pure organic connecting layer in tandem organic light emitting devices*"; Journal of the Electrochemical Society 257 (2010) H69–H71; http://dx.doi.org/10.1149/1.3247354

[11] M. Linares, D. Beljonne, J. Cornil, K. Lancaster, J.L. Brédas, S. Verlaak, A. Mityashin, P. Heremans, A. Fuchs, C. Lennartz, J. Idé, R. Méreau, P. Aurel, L. Ducasse, F. Castet; "*On the interface dipole at the pentacene-fullerene heterojunction: A theoretical study*"; The Journal of Physical Chemistry C 114 (2010) 3215–3224; http://dx.doi.org/10.1021/jp910005g

[12] M. Nakao, T. Manaka, M. Weis, E. Lim, M. Iwamoto; "*Probing carrier injection into pentacene field effect transistor by time-resolved microscopic optical second harmonic generation measurement*"; Journal of Applied Physics 106 (2009) 014511; http://doi.org/10.1063/1.3168434

[13] T. Manaka, M, Iwamoto; "*Optical second-harmonic generation measurement for probing organic device operation*"; Light: Science & Applications 5 (2016) e16040; http://dx.doi.org/10.1038/lsa.2016.40

[14] A. Pereira, S. Bonhommeau, S. Sirotkin, S. Desplanche, M. Kaba, C. Constantinescu, A.K. Diallo, D. Talaga, J. Penuelas, C. Videlot-Ackermann, A.P. Alloncle, P. Delaporte, V. Rodriguez; "*Morphological and crystalline characterization of pulsed laser deposited pentacene thin films for organic transistor applications*"; Applied Surface Science 418 (2017) 446–451; http://dx.doi.org/10.1016/j.apsusc.2017.01.281

[15] J.K. Lee, J.M. Koo, S.Y. Lee, T.Y. Choi, J. Joo, J.Y. Kim, J.H. Choi; "*Studies of pentacene-based thin film devices produced by cluster beam deposition methods*"; Optical Materials 21 (2003) 451-454; http://doi.org/10.1016/S0925-3467(02)00181-7

[16] J. Puigdollers, C. Voz, A. Orpella, I. Martin, M. Vetter, R. Alcubilla; "*Pentacene thin-films obtained by thermal evaporation in high vacuum*"; Thin Solid Films 427 (2003) 367-370; http://dx.doi.org/10.1016/S0040-6090(02)01238-5

[17] A.K. Diallo, R. Kurihara, N. Yoshimoto, C. Videlot-Ackermann; "*Morphology and microstructure of picene thin-films for air-operating transistors*"; Applied Surface Science 314 (2014) 704-710; http://doi.org/10.1016/j.apsusc.2014.07.085

[18] G.B. Blanchet, C. Fincher, I. Malajovich; "*Laser evaporation and the production of pentacene films*"; Journal of Applied Physics 94 (2003) 6181-6184; http://dx.doi.org/10.1063/1.1601681

[19] A.J. Salih, S.P. Lau, J.M. Marshall; "*Improved thin films of pentacene via pulsed laser deposition at elevated substrate temperatures*"; Applied Physics Letters 69 (1996) 2231; https://doi.org/10.1063/1.117137

[20] S. Ochiai, K. Palanisamy, S. Kannappan, P.K. Shin; "*Pentacene Active Channel Layers Prepared by Spin-Coating and Vacuum Evaporation Using Soluble Precursors for OFET Applications*"; ISRN Condensed Matter Physics (2012) ID 313285; http://dx.doi.org/10.5402/2012/313285

[21] H. Minemawari, T. Yamada, T. Hasegawa; "*Crystalline film growth of TIPS-pentacene by double-shot inkjet printing technique*"; Japanese Journal of Applied Physics 53 (2014) 05HC10; https://doi.org/10.7567/JJAP.53.05HC10

[22] T. Toccoli, P. Bettotti, A. Cassinese, S. Gottardi, Y. Kubozono, M.A. Loi, M. Manca, R. Verucchi; "*Photophysics of Pentacene-Doped Picene Thin Films*"; The Journal of Physical Chemistry C 122 (2018) 16879–16886; http://dx.doi.org/10.1021/acs.jpcc.8b02978

[23] L. Zhang, S. Huo, X. Fu, M. Hohage, L. Sun; "*Kinetic Barrier Against Standing Up of Pentacene Molecules Upon a Pentacene Monolayer*"; Physica Status Solidi - Rapid Research Letters 12 (2018) 1800230; http://dx.doi.org/10.1002/pssr.201800230

[24] I. Kaur, W. Jia, R.P. Kopreski, S. Selvarasah, M.R. Dokmeci, C. Pramanik, N.E. McGruer, G.P. Miller; "*Substituent Effects in Pentacenes: Gaining Control over HOMO−LUMO Gaps and Photooxidative Resistances*"; Journal of the American Chemical Society 130 (2008) 16274–16286; http://dx.doi.org/10.1021/ja804515y

[25] P. Delaporte, A. Ainsebaa, A.P. Alloncle, M. Benetti, C. Boutopoulos, D. Cannata, F. Di Pietrantonio, V. Dinca, M. Dinescu, J. Dutroncy, R. Eason, M. Feinaugle, J.M. Fernández-Pradas, A. Grisel, K. Kaur, U. Lehmann, T. Lippert, C. Loussert, M. Makrygianni, I. Manfredonia, T. Mattle, J.L. Morenza, M. Nagel, F. Nüesch, A. Palla-Papavlu, L. Rapp, N. Rizvi, G. Rodio, S. Sanaur, P. Serra, J. Shaw-Stewart, C.L. Sones, E. Verona, I. Zergioti; "*Applications of laser printing for organic electronics*"; SPIE Proceedings 8607 (2013) 86070Z; http://dx.doi.org/10.1117/12.2004062

[26] M. Girtan, S. Dabos-Seignon, A. Stanculescu; "*On morphological, structural and electrical properties of vacuum deposited pentacene thin films*"; Vacuum 83 (2009) 1159–1163; http://dx.doi.org/10.1016/j.vacuum.2009.03.001

[27] I. Stenger, A. Frigout, D. Tondelier, B. Geffroy, R. Ossikovski, Y. Bonnassieux; "*Polarized micro-Raman spectroscopy study*"; Applied Physics Letters 94 (2009) 133301; http://dx.doi.org/10.1063/1.3106053

[28] F. Anger, J.O. Ossó, U. Heinemeyer, K. Broch, R. Scholz, A. Gerlach, F. Schreiber; "*Photoluminescence spectroscopy of pure pentacene, perfluoropentacene, and mixed thin films*"; The Journal of Chemical Physics 136 (2012) 054701; http://dx.doi.org/10.1063/1.3677839

[29] Y. Zeng, B. Tao, J. Chen, Z. Yin; "*Temperature-dependent orientation study of the initial growth of pentacene on amorphous SiO_2 by molecular dynamics simulations*"; Journal of Crystal Growth 429 (2015) 35–42; http://dx.doi.org/10.1016/j.jcrysgro.2015.07.033

[30] F. Du, H. Huang; "*A generalized theory of thin film growth*"; Surface Science 669 (2018) 154–159; http://dx.doi.org/10.1016/j.susc.2017.12.002

[31] A. Winkler; "*On the nucleation and initial film growth of rod-like organic molecules*"; Surface Science 652 (2016) 367–377; http://dx.doi.org/10.1016/j.susc.2016.02.015

[32] H. Uoyama, H. Yamada, T. Okujima, H. Uno; "*Pentacene precursors for solution-processed OFETs*"; Tetrahedron 66 (2010) 6889–6894; http://dx.doi.org/10.1016/j.tet.2010.06.051

[33] T. Minakata, Y. Natsume; "*Direct formation of pentacene thin films by solution process*"; Synthetic Metals 153 (2005) 1–4; http://dx.doi.org/10.1016/j.synthmet.2005.07.210

[34] Y. Kim, D. Jeon; "*Real time monitoring of ordering in pentacene films during growth by using in-situ infrared spectroscopy*"; Current Applied Physics 17 (2017) 972–975; http://dx.doi.org/10.1016/j.cap.2017.04.001

[35] K. Itaka, T. Hayakawa, J. Yamaguchi, H. Koinuma; "*Pulsed laser deposition of c* axis oriented pentacene films*"; Applied Physics A 79 (2004) 875–877; http://dx.doi.org/10.1007/s00339-004-2793-9

[36] R. McGill, D. Chrisey; "*Method of Producing a Film Coating by Matrix assisted Pulsed Laser Deposition*", US Patent Number: 6025036, Issue Date: February 15th 2000

[37] E.J. Houser, D. Chrisey, M. Bercu, N.D. Scarisoreanu, A. Purice, D. Colceag, C. Constantinescu, A. Moldovan, M. Dinescu, "*Functionalized polysiloxane thin films deposited by matrix-assisted pulsed laser evaporation for advanced chemical sensor applications*"; Applied Surface Science 252 (2006) 4871-4876; http://dx.doi.org/10.1016/j.apsusc.2005.07.159

[38] A. Luches, A. Piqué, L.V. Zhigilei (Issue Editors): "*Matrix Assisted Pulsed Laser Evaporation: Fundamentals and Applications*"; Applied Physics A: Materials Science & Processing 105, issue 3 (2011) 517-701; ISSN: 0947-8396 (Print) 1432-0630 (Online)

[39] C. Constantinescu, N. Scarisoreanu, A. Moldovan, M. Dinescu, C. Vasiliu; "*Thin films of polyaniline deposited by MAPLE technique*"; Applied Surface Science 253 (2007) 7711-7714; http://doi.org/10.1016/j.apsusc.2007.02.057

[40] E. Morintale, C. Constantinescu, M. Dinescu; "*Thin films development by pulsed laser-assisted deposition*"; Physics AUC 20 (2010) 43-56;

[41] M. Tabetah, A. Matei, C. Constantinescu, N.P. Mortensen, M. Dinescu, J. Schou, L.V. Zhigilei; "*The Minimum Amount of "Matrix" Needed for Matrix-Assisted Pulsed Laser Deposition of Biomolecules*"; The Journal of Physical Chemistry B 118 (2014) 13290–13299; http://dx.doi.org/10.1021/jp508284n

[42] S. Brajnicov, A. Bercea, V. Marascu, A. Matei, B. Mitu; "*Shellac Thin Films Obtained by Matrix-Assisted Pulsed Laser Evaporation (MAPLE)*"; Coatings 8 (2018) 275; http://doi.org/10.3390/coatings8080275

[43] R. Birjega, A. Matei, B. Mitu, M.D. Ionita, M. Filipescu, F. Stokker-Cheregi, C.R. Luculescu, M. Dinescu, R. Zavoianu, O.D. Pavel, M.C. Corobea, "*Layered double hydroxides/polymer thin films grown by matrix assisted pulsed laser evaporation*"; Thin Solid Films 543 (2013) 63-68; http://dx.doi.org/10.1016/j.tsf.2013.02.120

[44] N.D. Scarisoreanu, F. Craciun, V. Ion, R. Birjega, A. Bercea, V. Dinca, M. Dinescu, L.E. Sima M. Icriverzi, A. Roseanu, L. Gruionu, G. Gruionu; "*Lead-Free Piezoelectric (Ba,Ca)(Zr,Ti)O3 Thin Films for Biocompatible and Flexible Devices*"; ACS Applied Materials & Interfaces 9 (2016) ; http://dx.doi.org/10.1021/acsami.6b14774

[45] V. Dinca, P.E. Florian, L.E. Sima, L. Rusen, C. Constantinescu, R.W. Evans, M. Dinescu, A. Roseanu; "*MAPLE-based method to obtain biodegradable hybrid polymeric thin films with embedded antitumoral agents*"; Biomedical Microdevices 16 (2014) 11-21; http://doi.org/10.1007/s10544-013-9801-9

[46] S.M. O'Malley, J. Tomko, A. Pérez del Pino, C. Logofatu, E. György; "*Resonant Infrared and Ultraviolet Matrix-Assisted Pulsed Laser Evaporation of Titanium Oxide/Graphene Oxide Composites: A Comparative Study*"; The Journal of Physical Chemistry C 118 (2014) 27911–27919; http://doi.org/10.1021/jp509067u

[47] M. Nagano, T. Hasegawa, N. Myoujin, J. Yamaguchi, K. Itaka, H. Fukumoto, T. Yamamoto, H. Koinuma; "*The First Observation of ^{1}H-NMR Spectrum of Pentacene*"; Japanese Journal of Applied Physics 43 (2004) L315; http://dx.doi.org/10.1143/JJAP.43.L315

[48] D. Knipp, R.A. Street, A. Völkel, J. Ho; "*Pentacene thin film transistors on inorganic dielectrics: Morphology, structural properties, and electronic transport*"; Journal of Applied Physics 93 (2003) 347; http://dx.doi.org/10.1063/1.1525068

[49] I.P.M. Bouchoms, W.A. Schoonveld, J. Vrijmoeth, T.M. Klapwijk; "*Morphology identification of the thin film phases of vacuum evaporated pentacene on SIO2 substrates*"; Synthetic Metals 104 (1999) 175-178; http://dx.doi.org/10.1016/S0379-6779(99)00050-8

[50] E.Z. Frażtczak, P. Uznanski, M.E. Moneta; "*Characterization of molecular organization in pentacene thin films on SiO_2 surface using infrared spectroscopy, spectroscopic ellipsometry,*

and atomic force microscopy", Chemical Physics 456 (2015) 49-56; http://doi.org/10.1016/j.chemphys.2015.04.015

[51] K.P. Weidkamp, C.A. Hacker, M.P. Schwartz, X. Cao, R.M. Tromp, R.J. Hamers; "*Interfacial Chemistry of Pentacene on Clean and Chemically Modified Silicon (001) Surfaces*"; The Journal of Physical Chemistry B 2003, 107, 11142-11148; http://dx.doi.org/10.1021/jp035385x

[52] Y. Hosoia, K. Okamura, Y. Kimura, H. Ishiia, M. Niwano; "*Infrared spectroscopy of pentacene thin film on SiO_2 surface*"; Applied Surface Science 244 (2005) 607–610; http://dx.doi.org/10.1016/j.apsusc.2004.10.131

[53] S. Berkebile, P. Puschnig, G. Koller, M. Oehzelt, F.P. Netzer, C. Ambrosch-Draxl, M.G. Ramsey; "*Electronic band structure of pentacene: An experimental and theoretical study*"; Physical Review B 77 (2008) 115312; http://dx.doi.org/10.1103/PhysRevB.77.115312

[54] R. Otero, A.L. Vázquez de Parga, J.M. Gallego; "*Electronic, structural and chemical effects of charge-transfer at organic/inorganic interfaces*"; Surface Science Reports 72 (2017) 105–145; http://dx.doi.org/10.1016/j.surfrep.2017.03.001

[55] I.S. Yahia, Y.S. Rammah, S. AlFaify, F. Yakuphanoglu; "*Optical characterization of nano-pentacene thin films*"; Superlattices and Microstructures 64 (2013) 58–69; http://dx.doi.org/10.1016/j.spmi.2013.08.022

[56] C.C. Shen, W.Y. Chou, H.L. Liu; "*Temperature dependence of optical properties of pentacene thin films probed by spectroscopic ellipsometry*"; Solid State Communications 188 (2014) 1–4; http://dx.doi.org/10.1016/j.ssc.2014.02.020

[57] G.F. Salem, E.A.A. El-Shazly, A.A.M. Farag, I.S. Yahia; "*Spectrophotometric investigations of optical linearity and nonlinearity of pentacene/ITO nanostructure thin film*"; Optik - International Journal for Light and Electron Optics 174 (2018) 221–233; https://doi.org/10.1016/j.ijleo.2018.08.018

[58] C. Constantinescu, L. Rapp, P. Rotaru, P. Delaporte, A.P. Alloncle; "*Pulsed laser processing of poly(3,3'''-didodecyl quarter thiophene) semiconductor for organic thin film transistors*"; Chemical Physics 450-451 (2015) 32–38; http://doi.org/10.1016/j.chemphys.2015.02.004

[59] E. Palik; "*Handbook of Optical Constants of Solids*", vol. 1; ISBN 9780080547213 (1985); Elsevier Inc., Academic Press, San Diego; http://doi.org/10.1016/C2009-0-20920-2

[60] D.A.G. Bruggeman; "*Berechnung verschiedener physikalischer Konstanten von heterogenen Substanzen. I. Dielektrizitätskonstanten und Leitfähigkeiten der Mischkörper aus isotropen Substanzen*"; Annalen der Physik 5 (1935) 636–662; http://dx.doi.org/10.1002/andp.19354160705

[61] L. Halagačka, K. Postava, J. Pištora; "*Analysis and Modeling of Depolarization Effects in Mueller Matrix Spectroscopic Ellipsometry Data*"; Procedia Materials Science 16 (2016) 112-117; http://doi.org/10.1016/j.mspro.2016.03.020

[62] H. Fujiwara, "*Spectroscopic Ellipsometry: Principles and Applications*"; John Wiley & Sons Ltd, Chichester (2007); ISBN 9780470016084 (print), ISBN 9780470060193 (online); http://doi.org/10.1002/9780470060193

[63] D. Faltermeier, D. Gompf, M. Dressel, A.K. Tripathi, J. Pflaum; "*Optical properties of pentacene thin films and single crystals*"; Physical Review B 74 (2006) 125416; http://doi.org/10.1103/PhysRevB.74.125416

[64] A.G. Gayathri, B.G. Sangeetha, C.M. Joseph; "*Optical studies on vacuum evaporated pentacene thin films on glass substrates*"; Materials Today: Proceedings 4 (2017) 584–589;

[65] T. Jentzsch, H.J. Juepner, K.W. Brzezinka, A. Lau; "*Efficiency of optical second harmonic generation from pentacene films of different morphology and structure*"; Thin Solid Films 315 (1998) 273–280; http://dx.doi.org/10.1016/S0040-6090(97)00797-9

[66] T. Jentzsch, H.J. Jüpner, S.H. Ashworth, T. Elsaesser; "*Second-order nonlinearities of polycrystalline molecular films studied on a 20-fs time scale*"; Optics Letters 21(1996) 492-494; http://doi.org/10.1364/OL.21.000492

[67] L.F. Drummy, P.K. Miska, D.C. Martin; "*Plasticity in pentacene thin films*"; Journal of Materials Science 39 (2004) 4465–4474; http://dx.doi.org/10.1023/B:JMSC.0000034139.73798.25

[68] A. Matei, M. Marinescu, C. Constantinescu, V. Ion, B. Mitu, I. Ionita, M. Dinescu, A. Emandi; "*Nonlinear optical studies on 4-(ferrocenylmethylimino)-2-hydroxy-benzoic acid thin films deposited by matrix-assisted pulsed laser evaporation (MAPLE)*"; Applied Surface Science 374 (2016) 206–212; http://dx.doi.org/10.1016/j.apsusc.2015.11.024

[69] V. Ion, A. Matei, C. Constantinescu, I. Ionita, M. Marinescu, M. Dinescu, A. Emandi; "*Octahydroacridine thin films grown by matrix-assisted pulsed laser evaporation for nonlinear optical applications*"; Materials Science in Semiconductor Processing 36 (2015) 78–83; http://dx.doi.org/10.1016/j.mssp.2015.02.064

Table & Figure captions

Table 1. Spectroscopic-ellipsometry parameters, where “Amp” is the amplitude of oscillation, “En” is the centre energy of oscillator, and “Br” is the broadening of the oscillator.

Figure 1. (a) MAPLE target holder and pentacene solution during liquid nitrogen cooling, and (b) FTIR spectra for pentacene dropcast vs. MAPLE deposited films, for different laser fluences (inset, upper left: the pentacene molecule)

Figure 2. (a) AFM and (b) SEM images on a pentacene thin film grown at 266 nm laser wavelength, on Silicon substrates (72 000 pulses at 0.4 J/cm^2) from a 1 wt% pentacene in toluene frozen target

Figure 3. (a) Spectroscopic-ellipsometry data fitting with 4 Gauss oscillators, and (b) the corresponding depolarization curve

Figure 4. Wavelength dependence of the (a) refractive index and (b) the extinction coefficients, obtained by fitting the experimental data with a sum of 4 Gauss oscillators

Figure 5. $(\alpha E)^2$ vs. E for a MAPLE pentacene deposited film

Figure 6. The transmission spectrum for a 400 nm pentacene thin film deposited onto a quartz substrate (grown at 0.3J/cm^2 laser fluence)

Figure 7. Emission intensity for pentacene powder

Figure 8. Plot of the I (SHG) vs. P (incident) for thin film samples grown by MAPLE

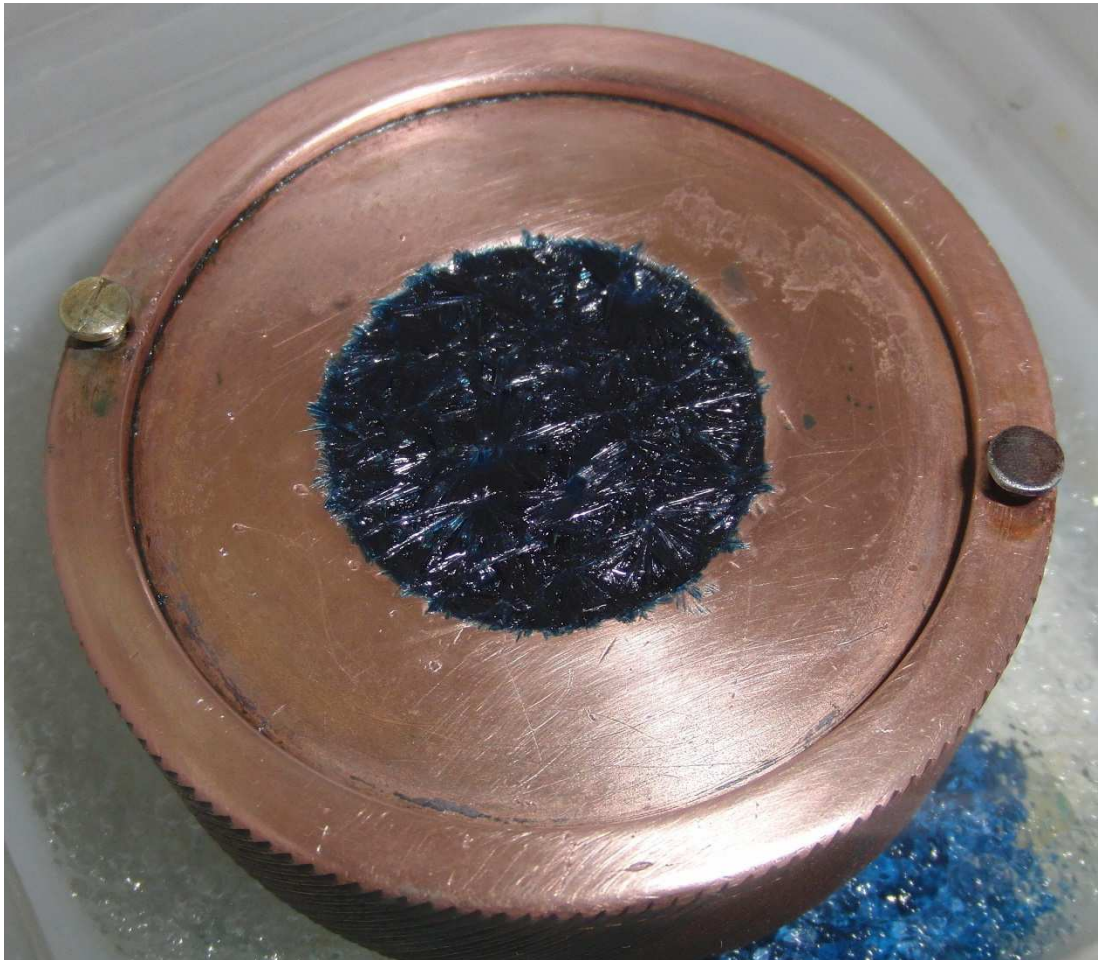

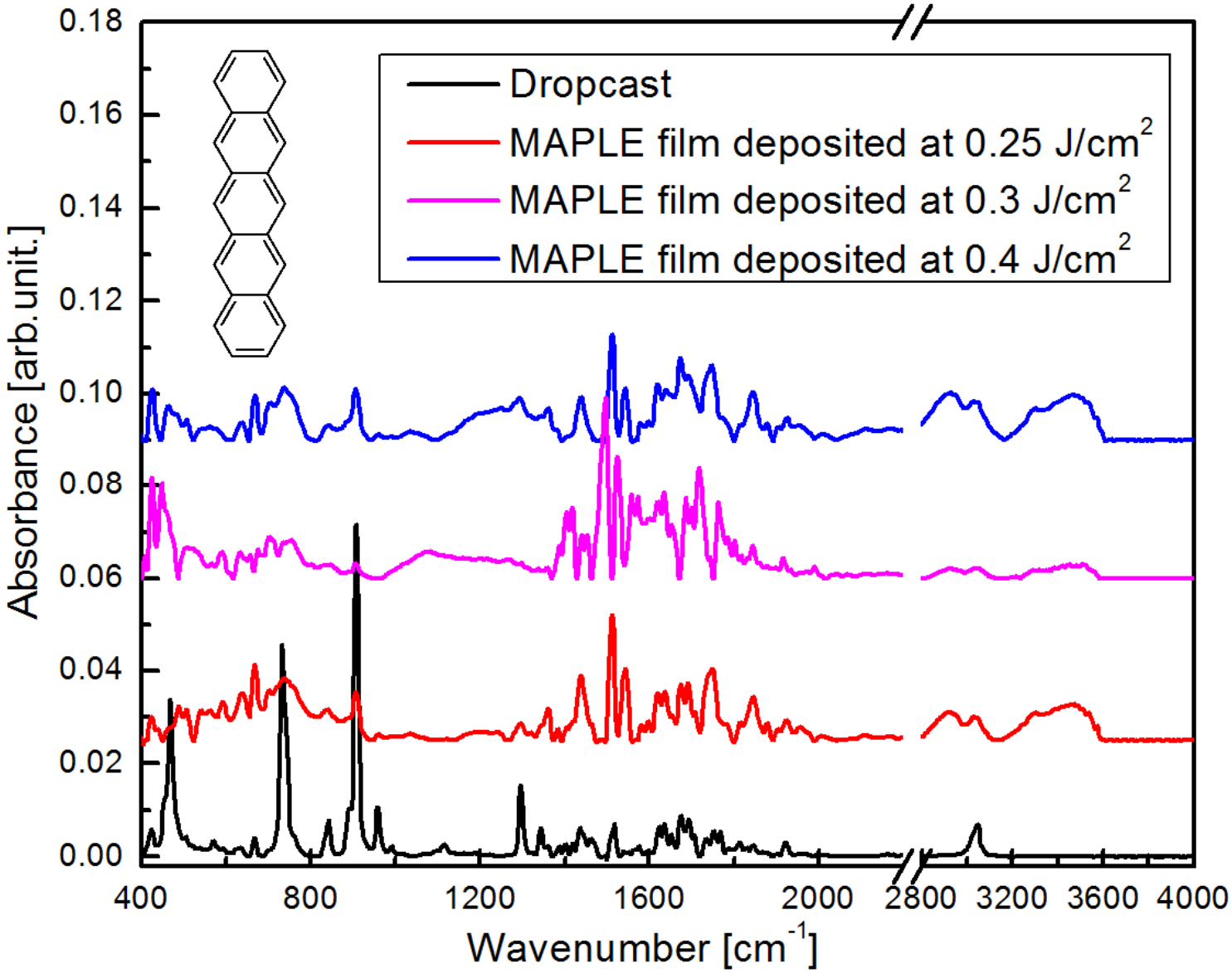
Dropcast
MAPLE film deposited at 0.25 J/cm2
MAPLE film deposited at 0.3 J/cm2
MAPLE film deposited at 0.4 J/cm2
Absorbance [arb.unit.]
0.18
0.16
0.14
0.12
0.10
0.08
0.06
0.04
0.02
0.00
400
800
1200
1600
2000
2800
3200
3600
4000
Wavenumber [cm-1]

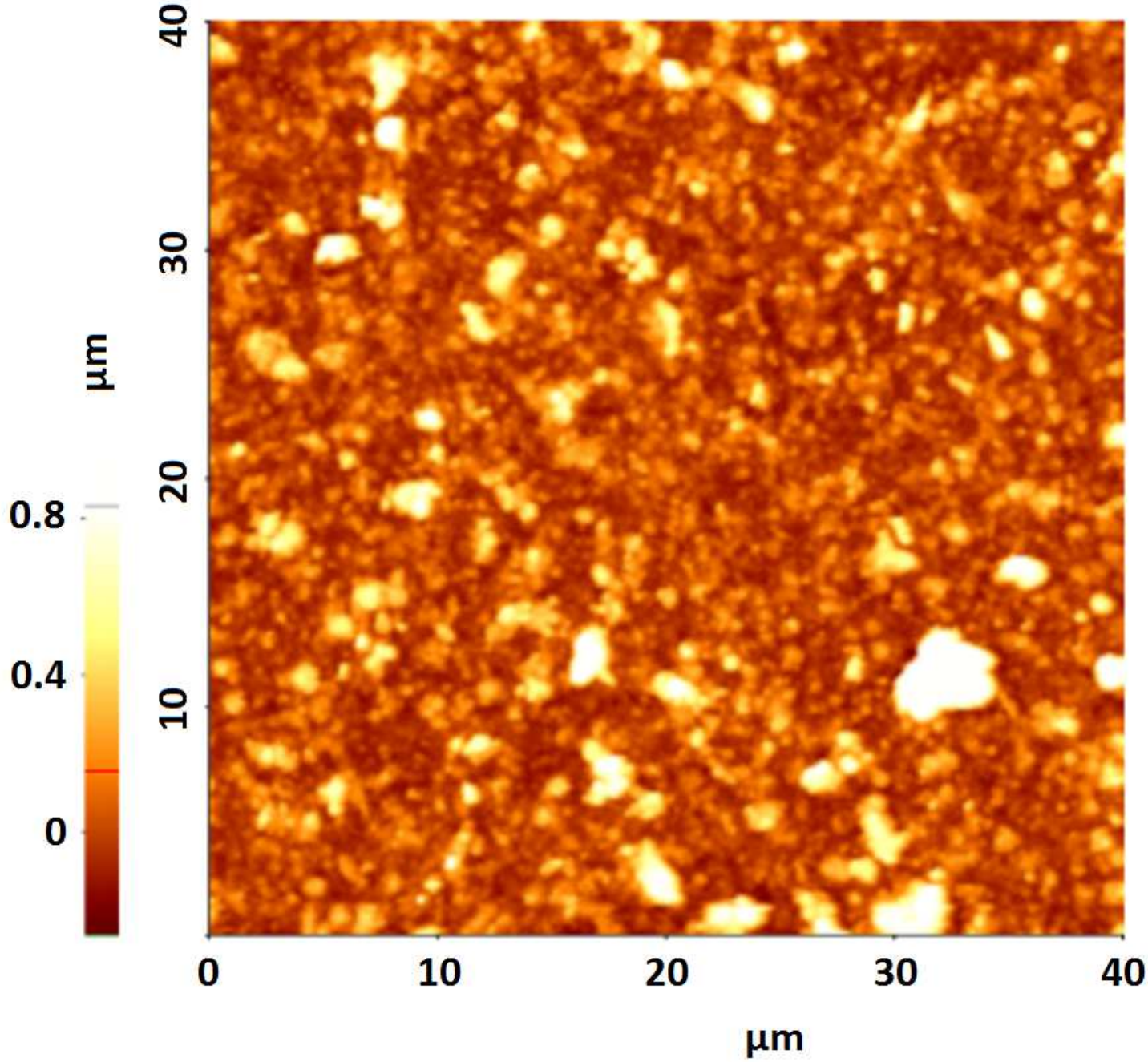
40
30
20
10
µm
0.8
0.4
0
0
10
20
30
40
µm

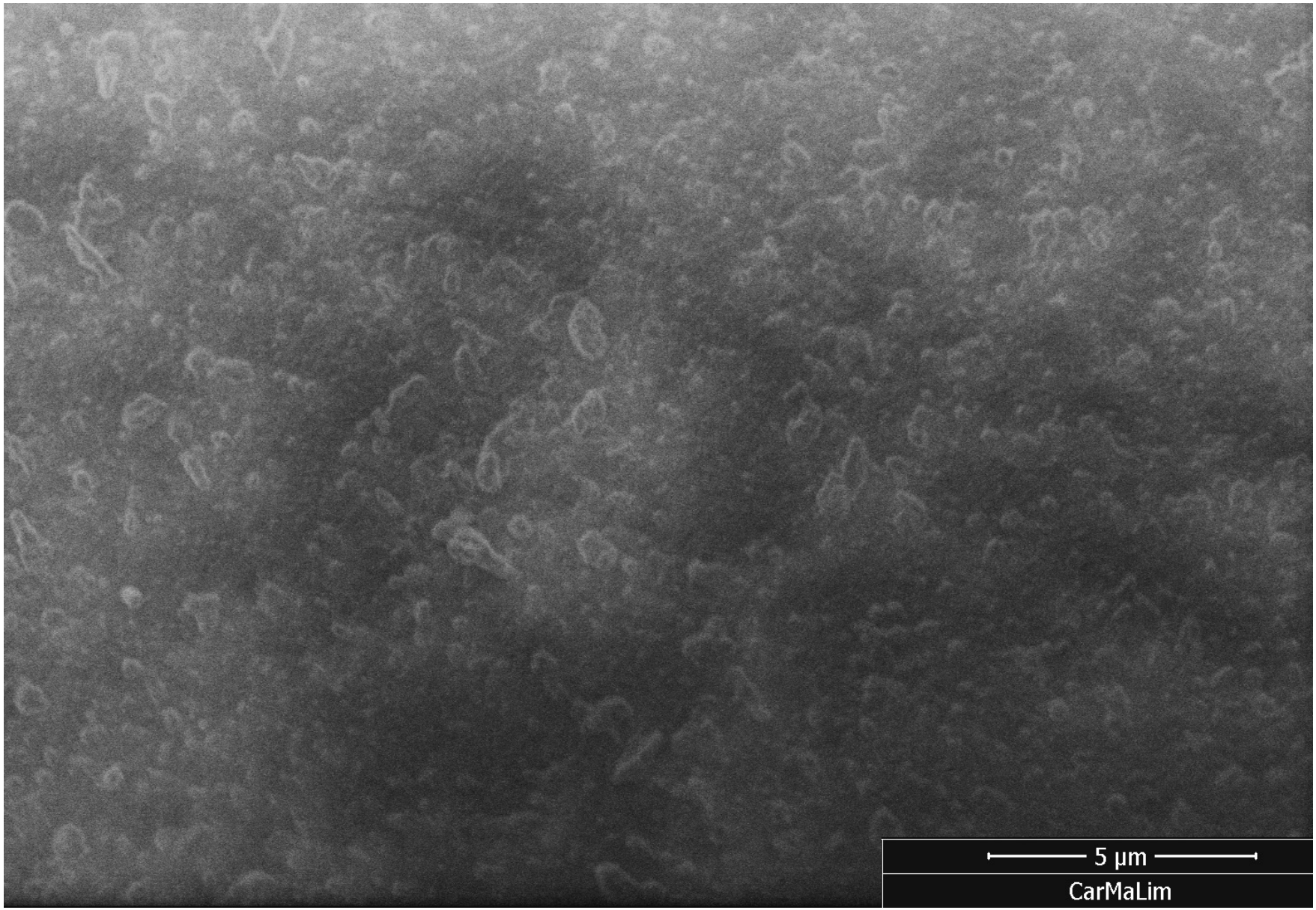
5 µm
CarMaLim

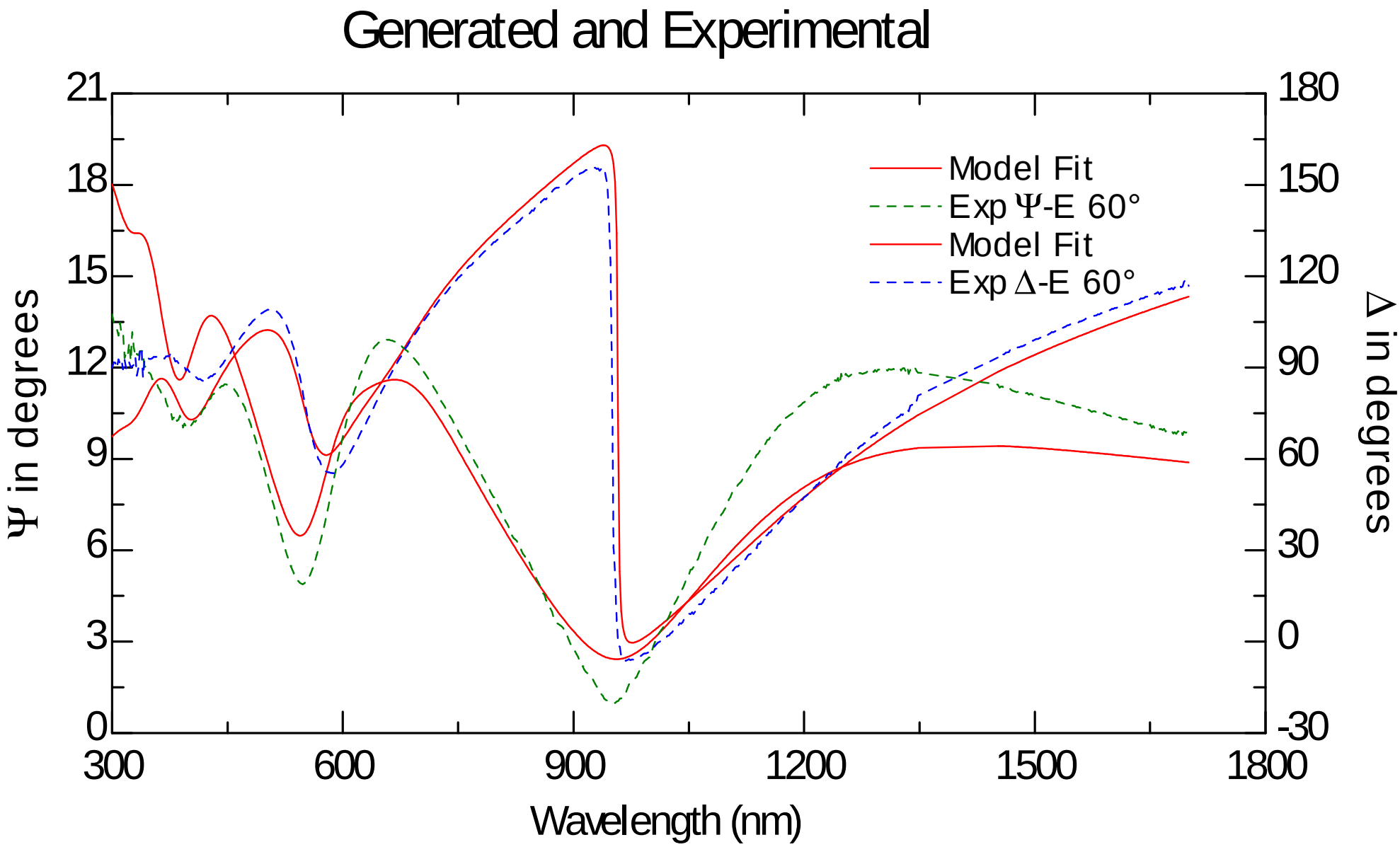
Generated and Experimental
Model Fit
Exp Ψ-E 60°
Model Fit
Exp Δ-E 60°
Ψ in degrees
Δ in degrees
Wavelength (nm)
0
3
6
9
12
15
18
21
-30
0
30
60
90
120
150
180
300
600
900
1200
1500
1800

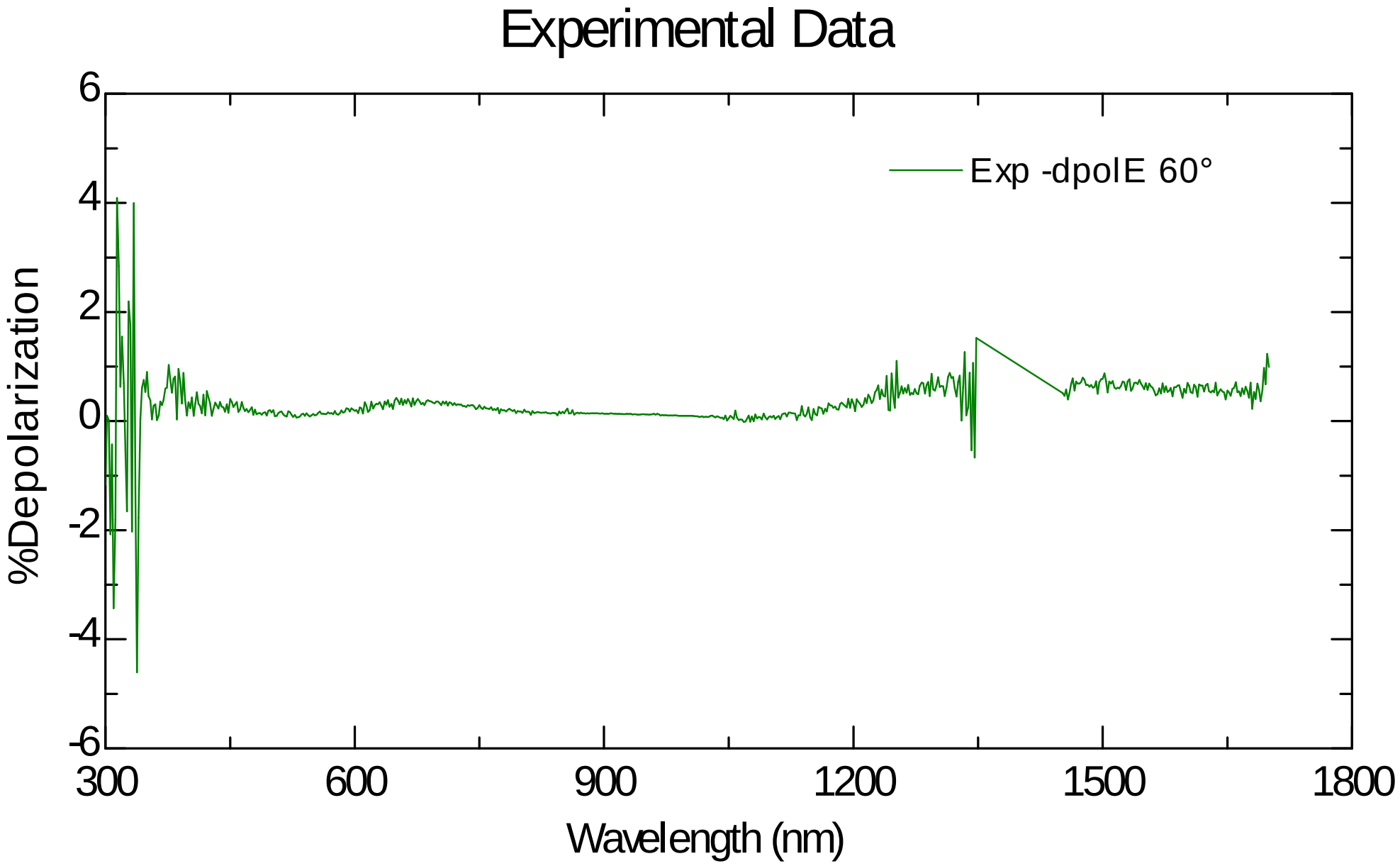
Experimental Data
Exp -dpolE 60°
%Depolarization
6
4
2
0
-2
-4
-6
300
600
900
1200
1500
1800
Wavelength (nm)

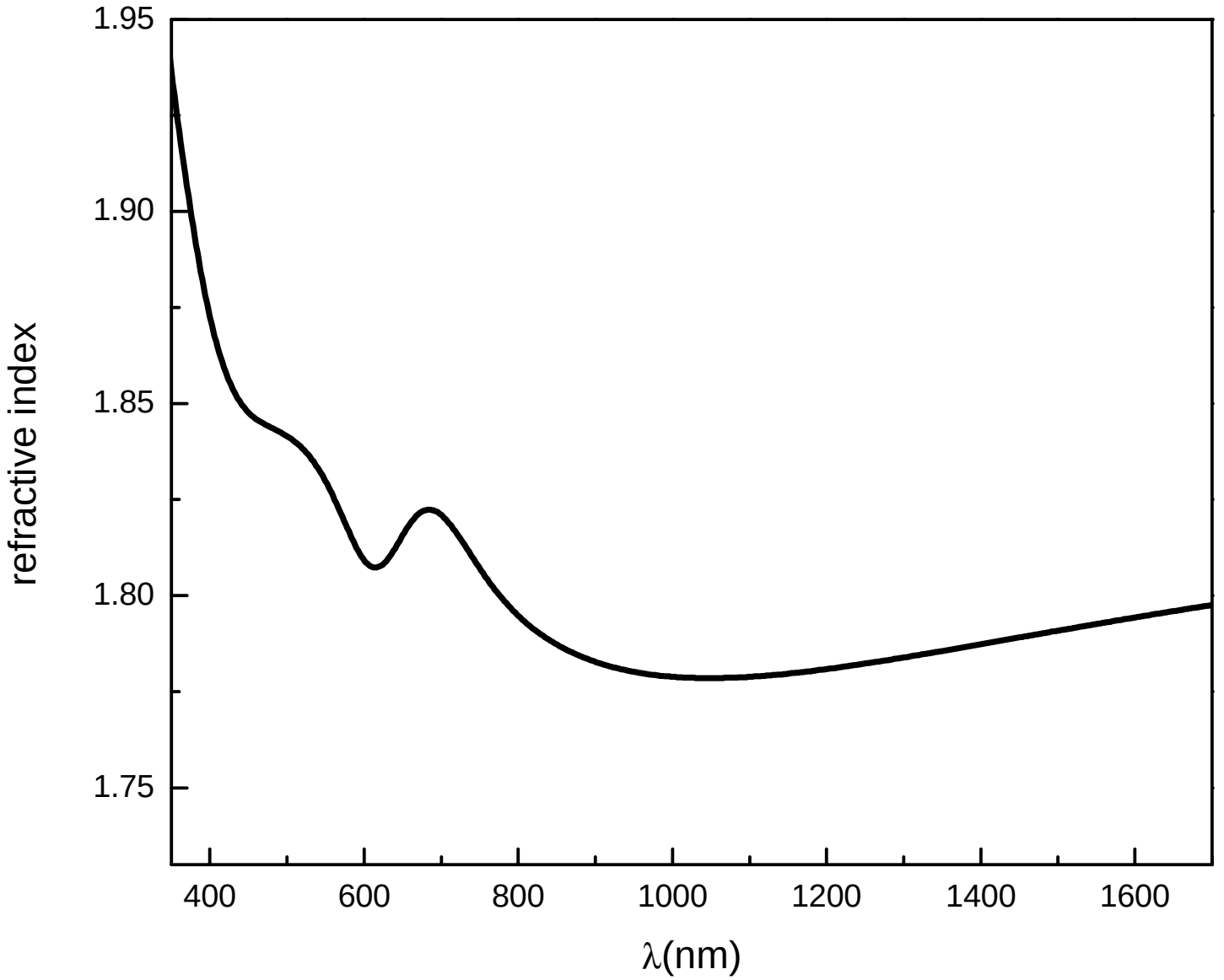
1.95
1.90
1.85
1.80
1.75
refractive index
400
600
800
1000
1200
1400
1600
λ(nm)

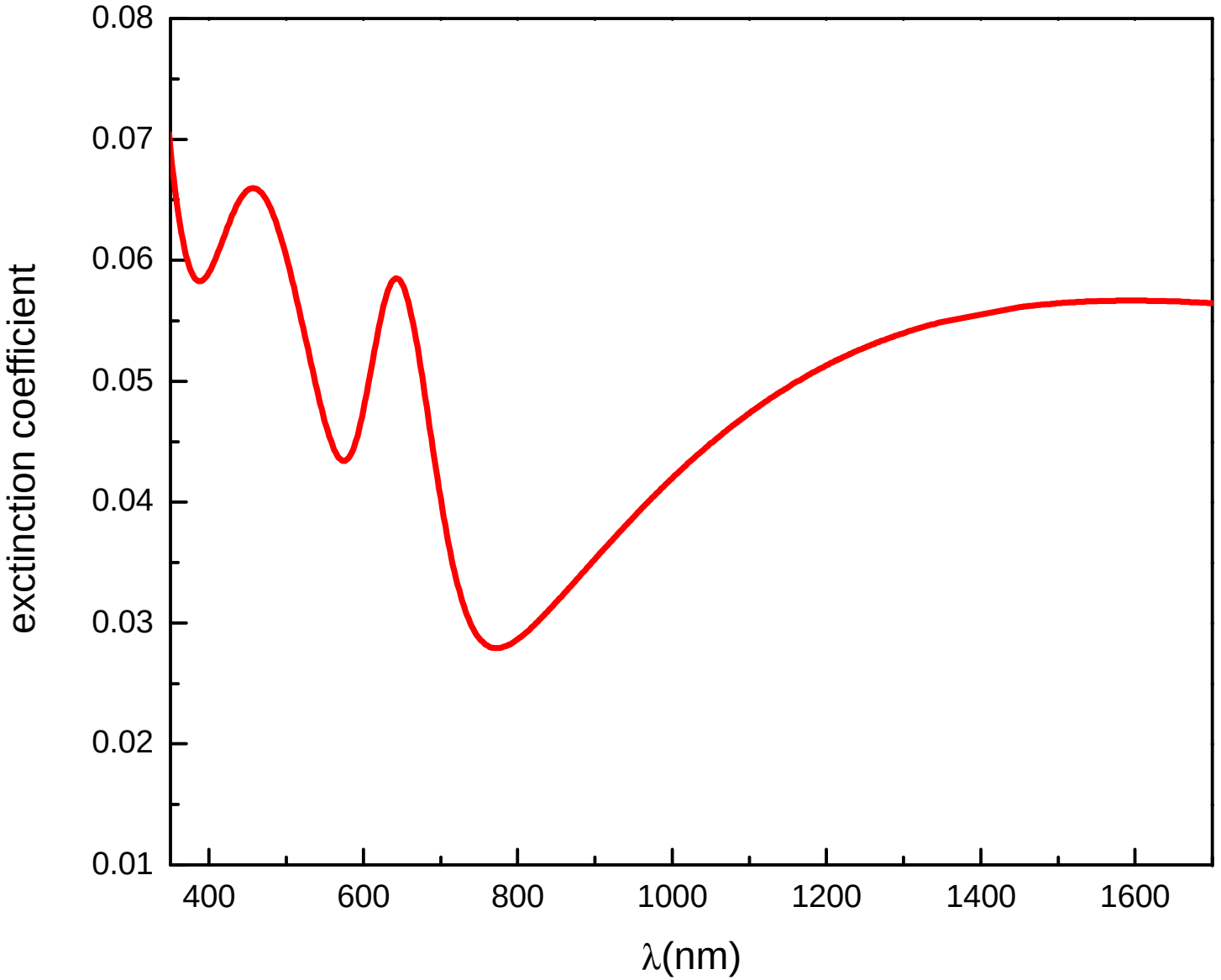
0.08
0.07
0.06
0.05
0.04
0.03
0.02
0.01
exctinction coefficient
400
600
800
1000
1200
1400
1600
λ(nm)

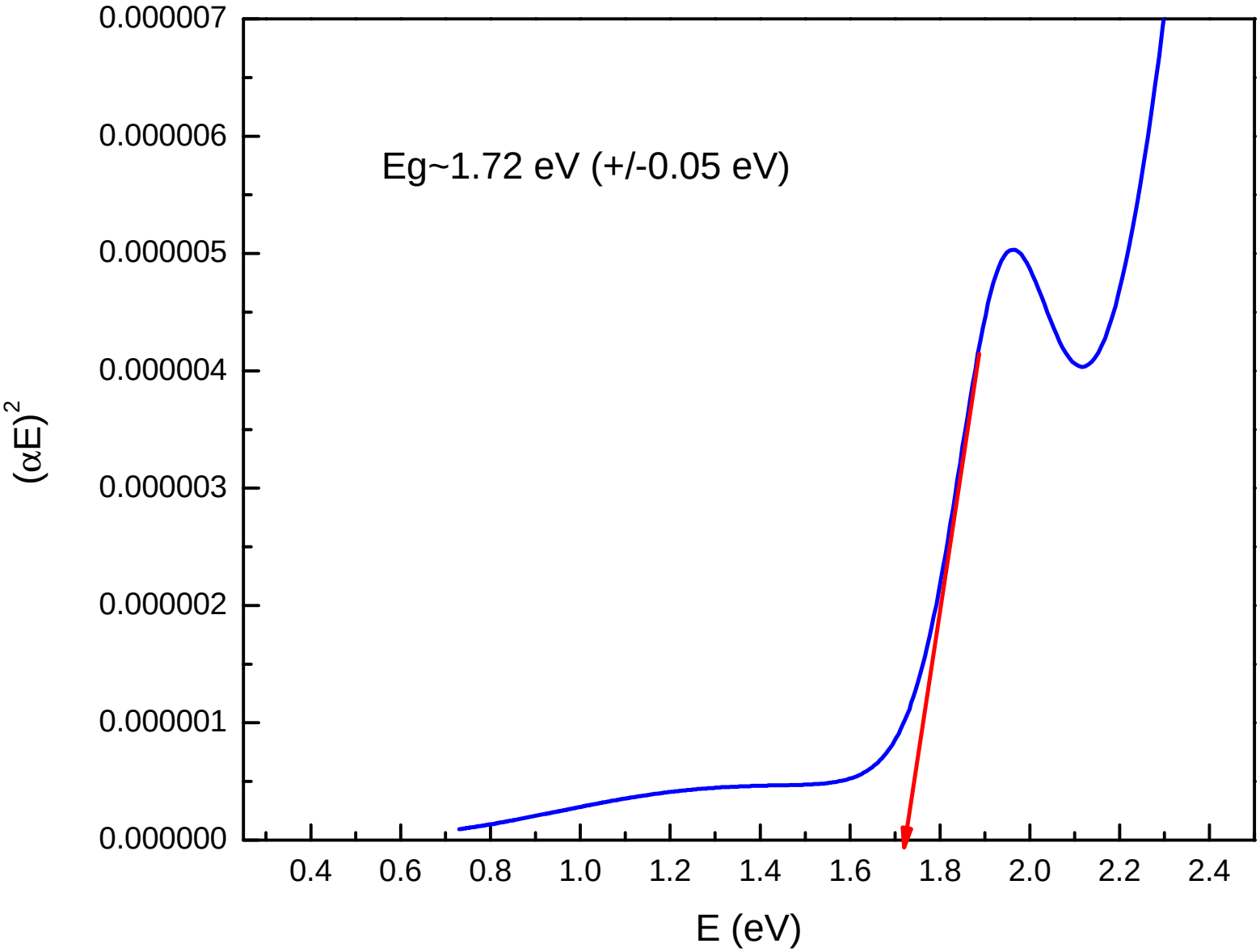
Eg~1.72 eV (+/-0.05 eV)
(αE)2
E (eV)
0.000000
0.000001
0.000002
0.000003
0.000004
0.000005
0.000006
0.000007
0.4
0.6
0.8
1.0
1.2
1.4
1.6
1.8
2.0
2.2
2.4

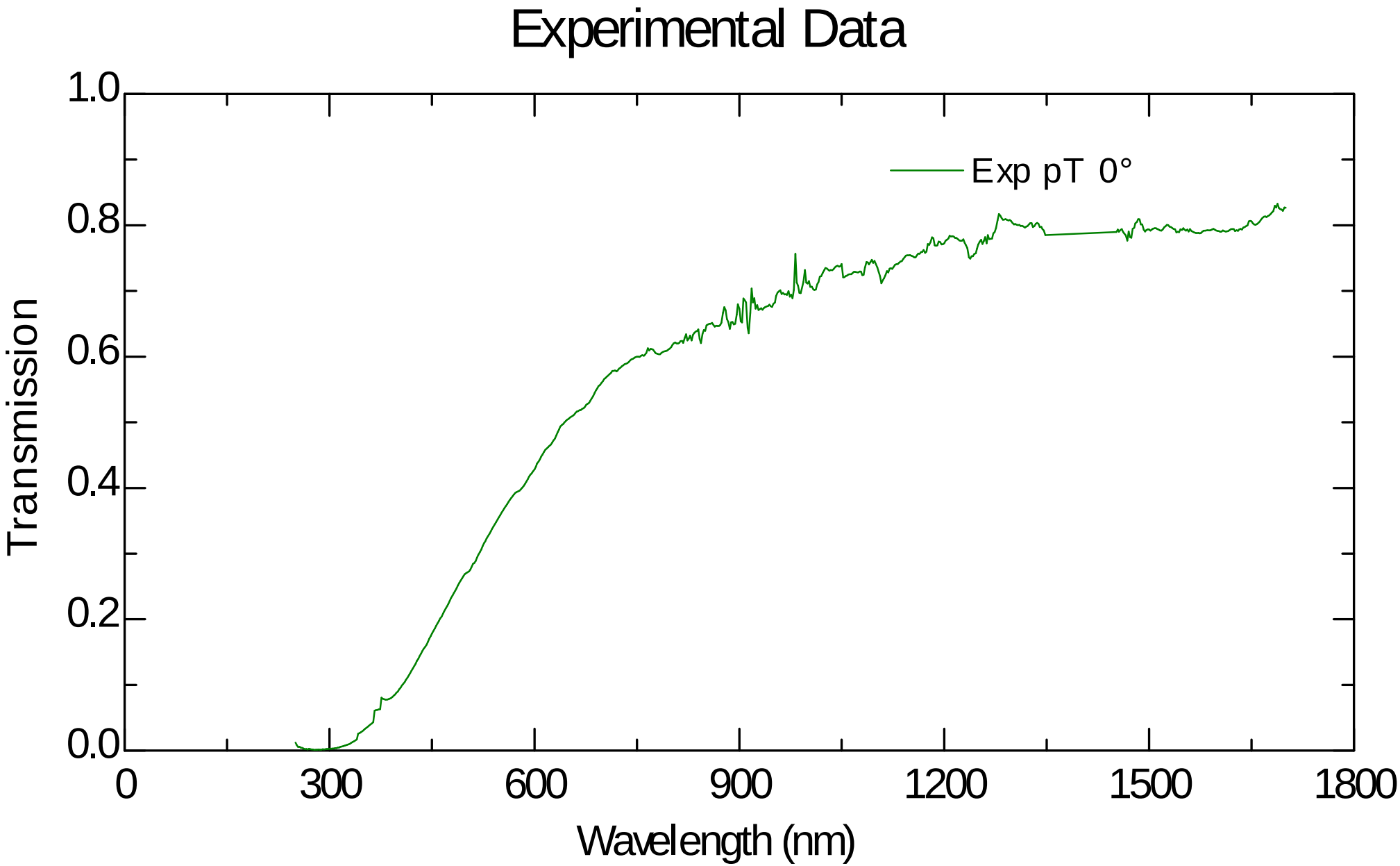
Experimental Data
Exp pT 0°
Transmission
Wavelength (nm)
1.0
0.8
0.6
0.4
0.2
0.0
0
300
600
900
1200
1500
1800

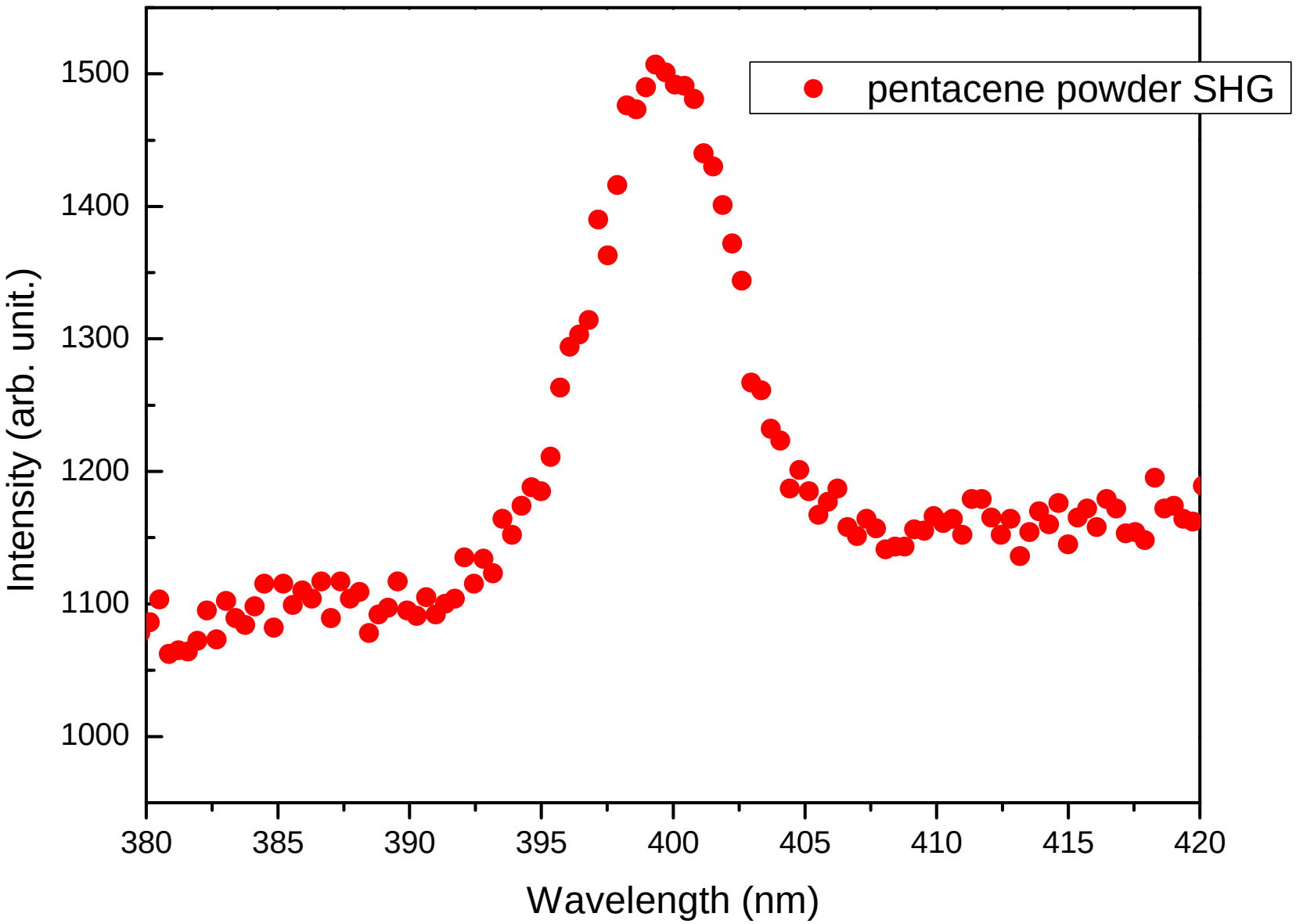
pentacene powder SHG
Intensity (arb. unit.)
1500
1400
1300
1200
1100
1000
380
385
390
395
400
405
410
415
420
Wavelength (nm)

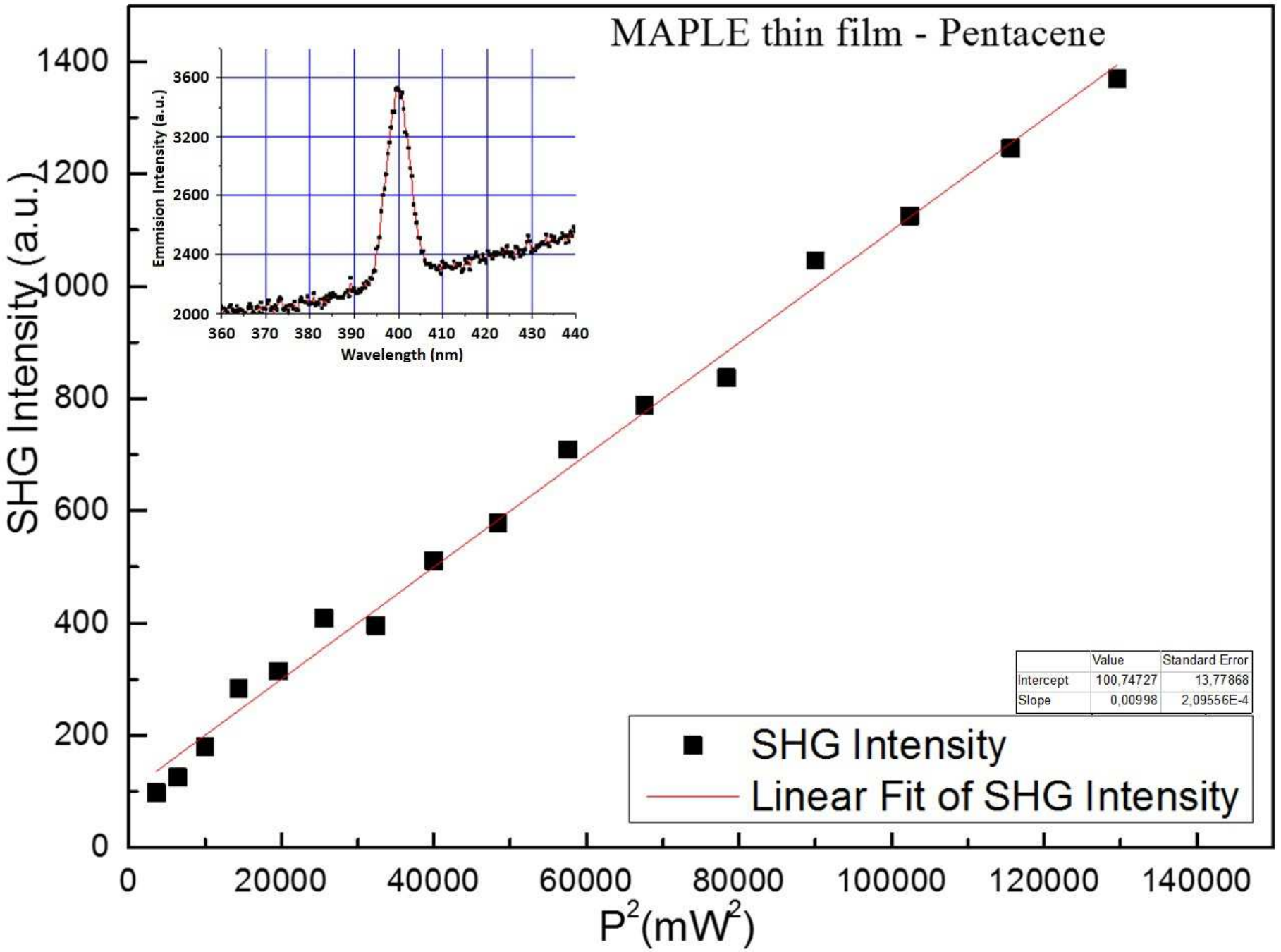
MAPLE thin film - Pentacene
SHG Intensity (a.u.)
P²(mW²)
0
200
400
600
800
1000
1200
1400
0
20000
40000
60000
80000
100000
120000
140000
Emmision Intensity (a.u.)
Wavelength (nm)
2000
2400
2600
3200
3600
360
370
380
390
400
410
420
430
440
Value
Standard Error
Intercept
100,74727
13,77868
Slope
0,00998
2,09556E-4
SHG Intensity
Linear Fit of SHG Intensity

No	Amp	En	Br
1	0.16797±0.038	2.5983±0.114	0.96713±0.39
2	0.11323±0.0422	1.9119±0.0461	0.28272±0.105
3	31.823±1.95	0.003947±0.000307	1.7852±0.12
4	5.2141±0.373	8.2306±0.102	4.496±0.314

Graphical Abstract